ISSN 1070-3284, Russian Journal of Coordination Chemistry, 2022, Vol. 48, No. 3, pp. 180–187. © Pleiades Publishing, Ltd., 2022.
Russian Text © The Author(s), 2022, published in Koordinatsionnaya Khimiya, 2022, Vol. 48, No. 3, pp. 185–192.

Rhenium Tris(pyrazolyl)borate Complexes with O-Donor Ligands: Synthesis and Structures

I. V. Skabitskii[a], * and S. S. Shapovalov[a]
[a] *Kurnakov Institute of General and Inorganic Chemistry, Russian Academy of Sciences, Moscow, 119991 Russia*
**e-mail: skabitskiy@gmail.com*

Received May 6, 2021; revised August 6, 2021; accepted August 7, 2021

Abstract—The reaction of $TpReOCl_2$ (Tp is the tris(pyrazolyl)borate anion) with methanol in the presence of triethylamine affords new rhenium alkoxide complex $TpReO(OMe)_2$ (**I**). Unlike the starting complex resistant to hydrolysis, complex **I** reacts with water in toluene to form the dimeric complex $[TpReO(\mu\text{-}O)]_2$ (**II**). The action of a large amount of water in acetone also leads to the decomposition of some Tp ligands and formation of the cationic complex $[(TpReO)_2(\mu\text{-}O)(\mu\text{-}C_3H_3N_2)]ReO_4$ (**III**) with the pyrazolate bridging ligand and perrhenate anion on the external sphere. The treatment of complex **I** with acetic anhydride gives the rhenium tris(pyrazolyl)borate complex bearing terminal acetate substituents $TpReO(OAc)_2$ (**IV**). The synthesized complexes are characterized by IR and NMR spectroscopy, and their structures are determined by X-ray diffraction (CIF files CCDC nos. 2081834 (**I**), 2081835 (**II**), 2081836 (**III**), 2081837 (**IV**)).

Keywords: rhenium complexes, alkoxide complexes, carboxylate complexes, tris(pyrazolyl)borate
DOI: 10.1134/S1070328422030046

INTRODUCTION

Tris(pyrazolyl)borate anions ($Tp^- = HB(C_3H_3N_2)_3^-$), being tridentate ligands and forming stable complexes with transition metals, found wide use in coordination chemistry [1]. Tris(pyrazolyl)borate anions are ligands of a weaker field, although they are often considered as analogs of cyclopentadienyl anions. Unlike diamagnetic ferrocenes, the corresponding complexes containing Tp^- are often high-spin [2]. In the case of rhenium, the complexes with the tris(pyrazolyl)borate ligands are known for the oxidation states from I to VIII, and the most studied types of these complexes are the $LReOX_2$ (L is $HBPz_3$ or BPz_4, Pz is pyrazolyl, and X is the monoanionic ligand) and $TpRe^I(CO)_3$ derivatives formed upon the substitution of one and more CO groups by various ligands [3]. The alkoxide complexes (X = OR) mainly with chelate alkoxide substituents compose an appreciable fraction among the Re(V) oxo complexes of the first type.

The alkoxide complexes $(BPz_4)ReO(OR)_2$ (R = Me, ^{i}Pp, Ph) and $(BPz_4)ReO(OXO)$ (X = CH_2CH_2, o-C_6H_4) were synthesized by the treatment of oxo-bridged $[(BPz_4)ReO(\mu\text{-}O)]_2$ with the corresponding alcohols [4]. The reaction of the bis(methylate) complex with diols was also used for the synthesis of complexes with bidentate alkoxides the chelate cycle size of which ranges from 5 to 7 (X = $CHMeCH_2$, CHMeCHMe, CMe_2CMe_2, $CH_2CH_2CH_2$, C_6H_{10}, and $CH_2CH_2CH_2CH_2$), which can be synthesized by the one-pot synthesis from $KBPz_4(PPh_3)_2ReCl_3O$ and corresponding diols [5]. An analogous complex $TpReO(OCHMeCH_2O)$ was synthesized by the treatment of $TpReOCl_2$ with $HOCHMeCH_2OH$ in the presence of triethylamine in acetonitrile and isolated in the enantiomerically pure form as a potential object to observe parity violation by spectroscopic methods [6]. The diolate complexes of anhydroerythrite and methyl-β-D-galactopyranose derivatives were synthesized under similar conditions but using methanol as the solvent [7]. The formation of the phenolate complexes TpReOCl(OPh) and $TpReO(O_2C_6H_4)$ was also observed for the oxidation of the phenyl group on the rhenium atom in TpReOPh(OTf) with pyridine oxide [8].

Unlike the alkoxide complexes, the carboxylate derivatives of rhenium tris(pyrazolyl)borate are restricted by several examples. The oxalate complex $TpReO(C_2O_4)$ (Scheme 1) was synthesized by the treatment of $TpReO(OCH_2CH_2O)$ with oxalic acid in acetonitrile [9]. The photochemical transformations of this complex related to the formation of the TpReO intermediate upon the photochemical elimination of the oxalate ligand [9]. The second example is represented by the complexes with the carboxylate–alkoxide ligand $LReO(Ph_2C(O)COO)$ (Scheme 1) formed due to the addition of diphenyl ketene to $LReO_3$ (L = Tp, $PhBPz_3$) [10].

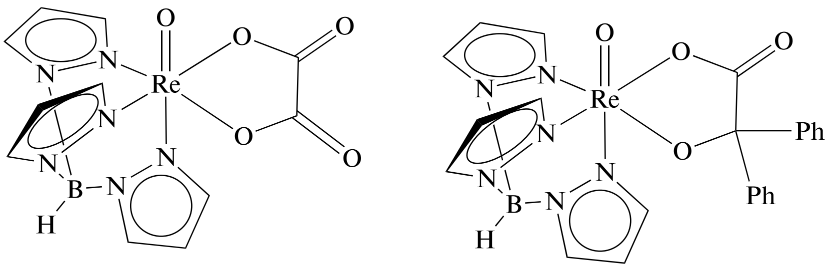

Scheme 1.

The tris(pyrazolyl)borate Re(V) oxo complexes containing methylate and acetate substituents were synthesized and their hydrolysis products were characterized in this work.

EXPERIMENTAL

All procedures on the synthesis and isolation of the products were carried out in absolute solvents under a pure argon atmosphere. IR spectra were recorded on a Bruker Alpha spectrometer equipped with a Bruker ATR Diamond ATR accessory. ^{1}H and ^{13}C NMR spectra were detected on a Bruker AV 300 instrument, and chemical shifts are presented relative to tetramethylsilane. Commercial triethylamine and acetic anhydride were used as received. The synthesis of $TpReOCl_2$ was carried out according to a published procedure [11].

Synthesis of $TpReO(OMe)_2$ (I). Triethylamine (235 μL, 1.7 mmol) was added to a suspension of $TpReOCl_2$ (408 mg, 0.84 mmol) in methanol (60 mL). The reaction mixture was stirred at 50°C overnight, and the obtained transparent blue solution was concentrated to 1/4 volume. The blue crystals of **I**·MeOH precipitated upon storing at –25°C were decanted, washed with methanol cooled to –80°C, and dried in vacuo. The yield was 374 mg (87%).

IR (ν, cm^{-1}): 3289 br.vw, 3120 w, 3106 vw, 2916 br.vw, 2819 vw, 2804 vw, 2518 vw, 1504 w, 1435 vw, 1404 m, 1390 vw, 1312 s, 1207 s, 1161 vw, 1118 w, 1103 vw, 1072 vw, 1049 w, 1036 vw, 1017 s, 991 vw, 961 vs, 858 vw, 802 w, 789 vw, 768 s, 728 vw, 710 s, 672 vw, 653 m, 620 m, 560 w, 535 s.

^{1}H NMR ($CDCl_3$; 298 K; δ, ppm): 1.18 (q, $^3J_{H-H}$ = 5.5 Hz, 1H, MeO*H*), 3.44 (d, $^3J_{H-H}$ = 5.5 Hz, 3H, *Me*OH), 4.66 (s, 6H, *Me*O), 6.07 (t, $^3J_{H-H}$ = 2.2 Hz, 1H), 6.41 (t, $^3J_{H-H}$ = 2.2 Hz, 2H), 7.42 (dd, $^3J_{H-H}$ = 2.1 Hz, $^4J_{H-H} \approx$ 0.6 Hz, 1H), 7.60 (d, $^3J_{H-H}$ = 2.1 Hz, 1H), 7.75 (dd, $^3J_{H-H}$ = 2.5 Hz, $^4J_{H-H}$ ~ 0.6 Hz, 2H), 7.89 (d, $^3J_{H-H}$ = 2.1 Hz, 2H).

$^{13}C\{^1H\}$ NMR ($CDCl_3$; 298 K; δ, ppm): 50.93 (*Me*OH), 73.45 (OMe), 106.18, 107.82, 134.48, 137.97, 143.11, 147.34.

A sample of complex **I** containing no solvate methanol was obtained by heating **I**·MeOH in vacuo at 80°C for 20 min.

For $C_{11}H_{16}BN_6O_3Re$ (*FW* = 477)

Anal. calcd., %:	C, 27.68	H, 3.38	N, 17.60
Found, %:	C, 28.83	H, 3.43	N, 17.30

^{1}H NMR (toluene-d$_8$; 298 K; δ, ppm): 4.83 (s, 6H, *Me*O), 5.51 (t, $^3J_{H-H}$ = 2.2 Hz, 1H), 5.78 (t, $^3J_{H-H}$ = 2.3 Hz, 2H), 6.86 (d, $^3J_{H-H}$ = 2.5 Hz, 1H), 7.16 (d, $^3J_{H-H}$ = 2.4 Hz, 2H), 7.46 (d, $^3J_{H-H}$ = 2.1 Hz, 1H), 7.74 (d, $^3J_{H-H}$ = 2.2 Hz, 2H).

Synthesis of $[TpReO(\mu\text{-}O)]_2$ (II). A suspension of complex **I** (50 mg, 0.11 mmol) and water (200 μL) in toluene (30 mL) was kept in an ultrasonic bath for 20 min until the starting substance dissolved. A yellow-brown precipitate formed upon storing for 2 days was decanted, washed with toluene (2 mL), and dried in vacuo. The yield of compound **II** was 31 mg (65%).

For $C_{18}H_{20}B_2N_{12}O_4Re_2$ (*FW* = 853)

Anal. calcd., %	C, 25.07	H, 2.34	N, 19.49
Found, %	C, 25.55	H, 2.73	N, 19.50

IR (ν, cm^{-1}): 3108 br.w, 2532 vw, 1707 m, 1698 vw, 1505 m, 1430 vw, 1405 vs, 1392 vw, 1365 m, 1310 vs, 1282 w, 1208 vs, 1183 m, 1122 m, 1108 vw, 1077 vw, 1050 vs, 1025 m, 996 vw, 975 s, 896 br.vs, 814 vw, 763 m, 724 vw, 710 br.vs, 672 vw, 650 w, 612 m, 530 w, 498 w, 459 vw, 441 vw, 422 vw, 409 vw.

The crystals of **II**·$CDCl_3$ suitable for X-ray diffraction (XRD) were obtained by storing a solution of **I** for a week in $CDCl_3$ containing water traces.

Synthesis of $[(TpReO)_2(\mu\text{-}O)(\mu\text{-}C_3H_3N_2)]ReO_4 \cdot 2Me_2CO$ (III). A solution of complex **I** (100 mg, 0.22 mmol) in a mixture of water (2 mL) and acetone (30 mL) was kept at room temperature for a week. The formed large black crystals were decanted, washed with acetone (10 mL), and dried in vacuo. The yield of complex **III** was 37 mg (40%).

For $C_{27}H_{35}B_2N_{14}O_9Re_3$ (*FW* = 1280)

Anal. calcd., %	C, 25.34	H, 2.76	N, 15.32
Found, %	C, 24.45	H, 2.68	N, 15.80

^{1}H NMR (DMSO-d_6; 298 K; δ, ppm): 2.08 (Me_2CO), 4.63 (br.s, 2H, *H*B), 6.16 (t, $^3J_{H-H}$ = 2.2 Hz, 2H), 6.50 (d, $^3J_{H-H}$ = 2.3 Hz, 2H), 6.81, (t, $^3J_{H-H}$ = 2.4 Hz, 2H), 6.83 (t, $^3J_{H-H}$ = 2.3 Hz, 2H), 7.30 (t, $^3J_{H-H}$ = 2.5 Hz, 1H), 7.94 (d, $^3J_{H-H}$ = 2.2 Hz, 2H), 8.19 (d, $^3J_{H-H}$ = 2.3 Hz, 2H), 8.41 (d, $^3J_{H-H}$ = 2.4 Hz, 2H), 8.60 (d, $^3J_{H-H}$ = 2.3 Hz, 2H), 8.88 (d, $^3J_{H-H}$ = 2.1 Hz, 2H), 8.92 (d, $^3J_{H-H}$ = 2.6 Hz, 2H).

^{13}C{^{1}H} NMR (DMSO-d_6; 298 K; δ, ppm): 30.67 (*Me*$_2$CO), 106.82, 109.23, 109.86, 116.39, 136.80, 139.79, 141.50, 141.61, 145.61, 148.40, 151.28, 206.48 (Me$_2$*C*O).

IR (ν, cm^{-1}): 3855 vw, 3736 vw, 3650 vw, 3146 vw, 3121 vw, 3086 vw, 2531 br.vw, 2502 vw, 1504 m, 1404 w, 1388 s, 1307 s, 1210 vs, 1187 vw, 1124 vw, 1116 m, 1098 vw, 1072 vw, 1047 vs, 986 w, 948 vs, 918 vw, 859 vw, 817 w, 793 vw, 779 vw, 759 vs, 730 vw, 713 m, 678 vw, 655 w, 631 vw, 617 vs, 554 w, 452 vw, 440 vw.

Synthesis of TpReO(OAc)$_2$ (IV). A solution of complex **I** (50 mg, 0.11 mmol) and Ac_2O (0.5 mL, 5.29 mmol) in dichloromethane (20 mL) was stirred for 24 h. A blue-green reaction mixture was concentrated in vacuo to 1 mL and kept at –25°C for 1 h. The precipitated blue crystals of complex **IV** were washed with diethyl ether and dried in vacuo. The yield of complex **IV** was 23 mg.

The crystals of complex **IV** suitable for XRD were additionally obtained in an amount of 8 mg by the diffusion of diethyl ether vapors to the mother liquor for 3 days. The overall yield was 31 mg (53%).

For $C_{13}H_{16}BN_6O_5Re$ (*FW* = 533).

Anal. calcd., %	C, 29.28	H, 3.02	N, 15.76
Found, %	C, 29.23	H, 2.79	N, 15.86

^{1}H NMR ($CDCl_3$; 298 K; δ, ppm): 2.35 (s, 6H, *Me*COO), 6.08 (t, $^3J_{H-H}$ = 2.2 Hz, 1H), 6.47 (t, $^3J_{H-H}$ = 2.4 Hz, 2H), 7.41 (dd, $^3J_{H-H}$ = 2.2 Hz, $^4J_{H-H} \approx 0.6$ Hz, 1H), 7.85 (dd, $^3J_{H-H}$ = 2.5 Hz, $^4J_{H-H} \approx 0.6$ Hz, 2H), 8.00 (d, $^3J_{H-H}$ = 2.3 Hz, 2H), 8.15 (d, $^3J_{H-H}$ = 2.1 Hz, 1H).

^{13}C{^{1}H} NMR ($CDCl_3$, 298 K, δ ppm): 23.46 (OOC*Me*), 105.99, 108.53, 134.83, 139.13, 144.94, 148.46, 182.78 (OO*C*Me).

IR (ν, cm^{-1}): 3141 vw, 3121 vw, 3101 vw, 2539 br.vw, 1686 m, 1661 br.m, 1504 w, 1441 vw, 1404 m, 1361 m, 1312 w, 1283 br.s, 1243 w, 1210 m, 1186 vw, 1126 vw, 1116 w, 1084 vw, 1052 vs, 986 m, 913 w, 811 vw, 772 vs, 711 m, 680 vw, 670 vw, 647 s, 620 w, 602 vw, 565 vw, 543 w, 532 vw.

XRD was carried out on a Bruker APEX II CCD diffractometer for complexes **I** and **III** and on a Bruker Venture D8 diffractometer for complexes **II** and **IV**. An absorption correction was applied by multiple measuring equivalent reflections using the SADABS program [12]. The structures of compounds **I**–**IV** were solved by a direct method and refined by least squares against F^2 in the anisotropic approximation of non-hydrogen atoms using the SHELX-2014 [13] and OLEX2 [14] program packages. The positions of hydrogen atoms were calculated geometrically. The crystallographic data and structure refinement parameters for compounds **I**–**IV** are presented in Table 1. Selected bond lengths and bond angles in compounds **I**–**IV** are given in captions to Figs. 1–4.

The coordinates of atoms and other parameters for the structures of complexes **I**–**IV** were deposited with the Cambridge Crystallographic Data Centre (CIF files CCDC nos. 2081834–2081837, respectively; http://www.ccdc.cam.ac.uk/data_request/cif).

Quantum-chemical calculations were performed in the framework of the density functional theory using the ORCA 4.21 software [15]. The geometry optimization of the complexes and transition states was carried out using the PBE functional [16, 17] with the double-zeta all-electron def2-SVP basis set [18] and applying a D3BJ empirical correction to dispersion interactions [19, 20]. The activation energy was calculated using the PBE0 hybrid functional [21] with the triple-zeta all-electron def2-TZVP basis set [18].

RESULTS AND DISCUSSION

The treatment of $TpReOCl_2$ with triethylamine in boiling methanol gave new methoxide complex TpReO(OMe)$_2$ (**I**). Unlike the starting chloride complex resistant to hydrolysis, complex **I** slowly reacts with water: new oxo-bridged dimeric complex [TpReO(μ-O)]$_2$ (**II**) is formed in toluene upon the action of water. The treatment with a water excess in acetone also results in the cleavage of some tris(pyrazolyl)borate ligands with the formation of the cationic dimer [(TpReO)$_2$(μ-O)(μ-$C_3H_3N_2$)]ReO$_4$ (**III**) in which one of the oxygen bridging ligands was replaced by the pyrazolate ligand.

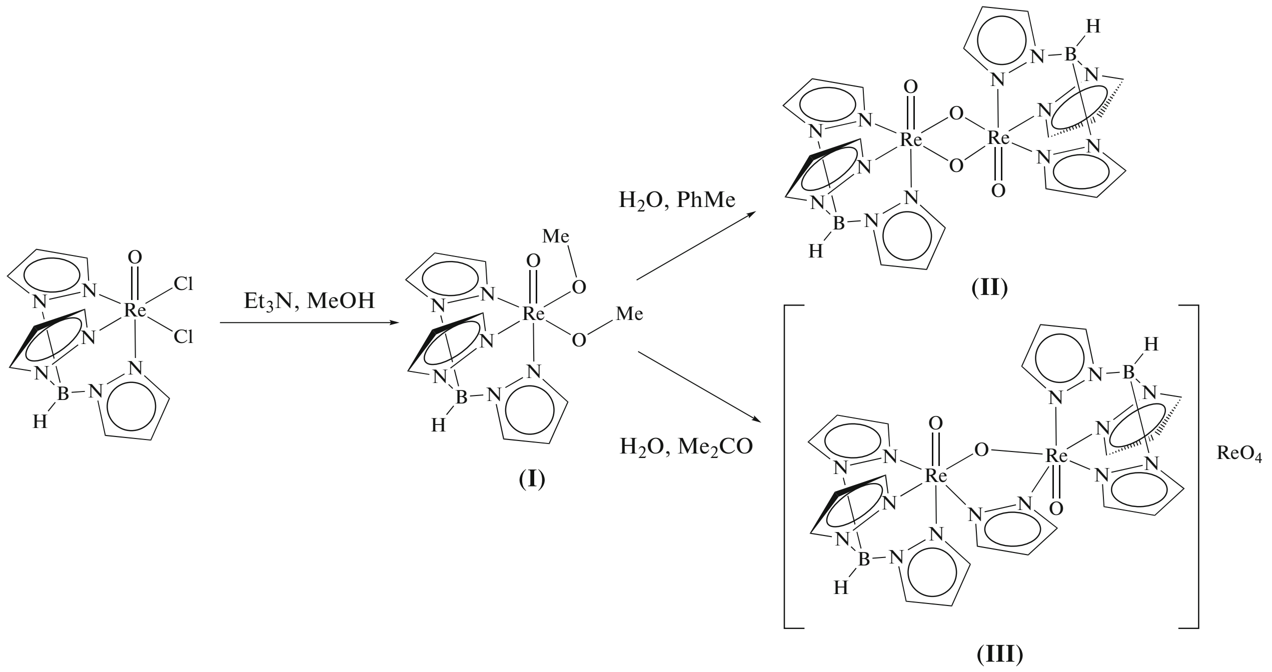

Scheme 2.

The structures of the complexes were determined by XRD. In particular, the molecular structure of complex **I** is shown in Fig. 1. The Re–O bonds with the methylate groups (1.969(5), 1.933(5) Å) are much longer than the multiple bond with the oxo ligand (1.684(5) Å) but is noticeably shorter than the sum of covalent radii (2.17 Å) [22]. This fact along with an increase in the ReOC angles (124.9(5)°) compared to the tetrahedral one indicates an appreciable additional Re–methylate bonding due to the donation of the lone pair of oxygen to the antibonding π orbital of the multiple Re–O bond with the oxo ligand. The Re–N distances for the nitrogen atom in the *trans* position to the methoxide (2.102(6), 2.145(5) Å) and oxygen (2.242(6) Å) ligands are noticeably nonequivalent, most likely, due to a stronger *trans* effect of the oxo ligand. The Re–N distances in the *trans* position to the methoxide groups are shorter, on the average, than the Re–N distances (2.147 and 2.175 Å) in the *trans* position to the thiolate substituents in the propyl–thiolate analog TpReO$(SC_3H_7)_2$ [23].

The structure of the TpRe fragment in oxo-bridged dimer **II** is similar to its structure in compound **I** (Fig. 2). The Re–N distances in the *trans* position to the terminal ligand are still more elongated (2.299(5) Å) compared to two others (2.100(2), 2.134(2) Å). The Re–O distances with the bridging oxygen atoms (1.948(2), 1.974(2) Å) are significantly longer than those with the terminal atoms (1.689(2) Å) and are nearly equivalent to the Re–O$_{Me}$ distances in the starting complex **I**. The Re...Re distance (3.1049(2) Å) turns out to be only slightly longer than the bonding Re–Re distance in rhenium carbonyl (3.042 Å). Such a short Re...Re contact is a consequence, most likely, of the geometry of the bridging ligands. However, an additional interaction of the lone pair on Re(V) with the antibonding π orbitals of the multiple Re–O bond on the adjacent rhenium atom cannot be excluded.

In cationic dimer **III** (Fig. 3), the substitution of one of the oxygen bridging ligands by pyrazolate results in an increase in the Re...Re distance to 3.51434 Å and in the ReORe angle to 130.5(3)°. However, the Re–O distances with the oxygen bridge are even somewhat shorter (1.924(6), 1.935(6) Å). The Re–N distances in the *trans* position to the pyrazolate bridge (2.046(5), 2.067(5) Å) are appreciably shorter than those in the *trans* position to the oxygen bridge (2.133(5), 2.159(5) Å).

The ^{1}H and ^{13}C NMR spectra of complex **I** exhibit one signal of the methyl groups and two sets of signals of pyrazolates in a ratio of 1 : 2 indicating that the nonequivalence of the methyl groups observed by XRD disappears in the solution. The hindered rotation of the thiolate groups with barriers of 13 and 12.6 kcal/mol (for R = CMe$_3$ and *n*-C$_3$H$_7$, respectively) was observed for analogous thiolate complexes TpReO(SR)$_2$ [23]. Therefore, it seemed interesting to study the temperature dependence of the ^{1}H NMR spectrum of complex **I** that demonstrates specific features of the structure similar to those of the thiolate complexes. However, the spectrum of complex **I** underwent no substantial changes up to 253 K, which indicates a lower rotation barrier of OMe compared to those for the thiolate substituents.

Table 1. Crystallographic data and structure refinement parameters for complexes **I**–**IV**

Parameter	**I**	**II**	**III**	**IV**
Empirical formula	$C_{12}H_{20}BN_6O_4Re$	$C_{20}H_{22}B_2N_{12}O_4Cl_6Re_2$	$C_{27}H_{35}B_2N_{14}O_9Re_3$	$C_{13}H_{16}BN_6O_5Re$
FW	509.35	1101.21	1279.91	533.33
Radiation (λ , Å)	MoK_α (λ = 0.71073)			
Recording temperature, K	296	100	150	100
Crystal system	Monoclinic	Monoclinic	Orthorhombic	Monoclinic
Space group	$P2_1/n$	$P2_1/c$	*Pbcn*	$P2_1/n$
a, Å	13.838(6)	7.7589(2)	28.7444(6)	7.5114(4)
b, Å	8.610(4)	20.2699(6)	15.6392(4)	16.3728(9)
c, Å	15.160(5)	10.4552(3)	16.9346(4)	13.6934(8)
α, deg	90	90	90	90
β, deg	104.580(13)	97.1230(10)	90	90.739(2)
γ, deg	90	90	90	90
V, Å^3	1748.1(12)	1631.62(8)	7612.8(3)	1683.91(16)
Z	4	2	8	4
ρ_{calc}, g/cm^{-3}	1.935	2.241	2.233	2.104
μ, mm^{-1}	6.980	7.954	9.585	7.256
F(000)	984.0	1040.0	4816.0	1024.0
Scan range, deg	4.606–59.84	5.62–60.016	4.538–54.378	3.878–57.346
Scan mode	ω			
Independent reflections (N_1)	4625 (R_{int} = 0.0739)	4752 (R_{int} = 0.0581)	8470 (R_{int} = 0.0727)	4330 (R_{int} = 0.0404)
Reflections with $I > 2\sigma(I)$ (N_2)	3475	4316	7706	3922
Number of refined parameters	225	209	501	240
GOOF (F^2)	1.067	1.085	1.251	1.090
R_1 for N_2	0.0509	0.0180	0.0418	0.0187
wR_2 for N_1	0.0942	0.0375	0.0675	0.0443
$\Delta\rho_{max}/\Delta\rho_{min}$, e Å^{-3}	1.20/–1.83	0.85/–0.84	1.06/–2.34	0.93/–0.72

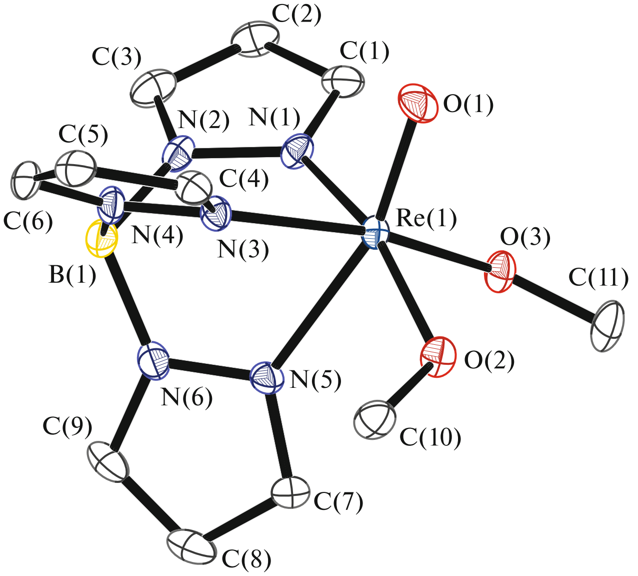

Fig. 1. Molecular structure of complex **I** (solvate methanol molecule is omitted). Selected bond lengths: Re(1)–O(1) 1.684(5), Re(1)–O(2) 1.933(5), Re(1)–O(3) 1.969(5), Re(1)–N(1) 2.102(6), Re(1)–N(3) 2.145(5), and Re(1)–N(5) 2.241(6) Å and bond angles: O(1)Re(1)O(2) 108.8(2)° O(1)Re(1)O(3) 103.7(2)°, O(2)Re(1)O(3) 85.6(2)°, C(10)O(2)Re(1) 124.9(4)°, and C(11)O(3)Re(1) 124.9(5)°.

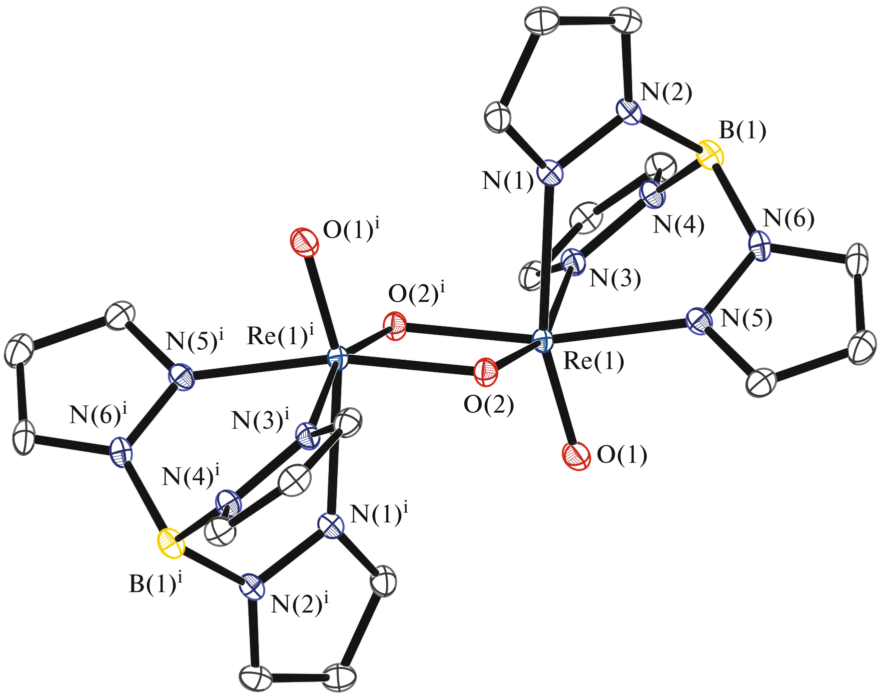

Fig. 2. Cationic moiety of the molecular structure of complex **II**. Selected bond lengths: Re(1)–Re(1)^{i} 3.1049(2), Re(1)–O(1) 1.689(2), Re(1)–O(2)^{i} 1.948(2), Re(1)–O(2) 1.974(2), Re(1)–N(1) 2.299(2), Re(1)–N(3) 2.100(2), and Re(1)–N(5) 2.134(2) Å and bond angles: O(1)Re(1)O(2) 104.18(8)°, O(1)Re(1)O(2)^{i} 107.52(8)°, and Re(1)^{i}O(2)Re(1) 104.70(8)°.

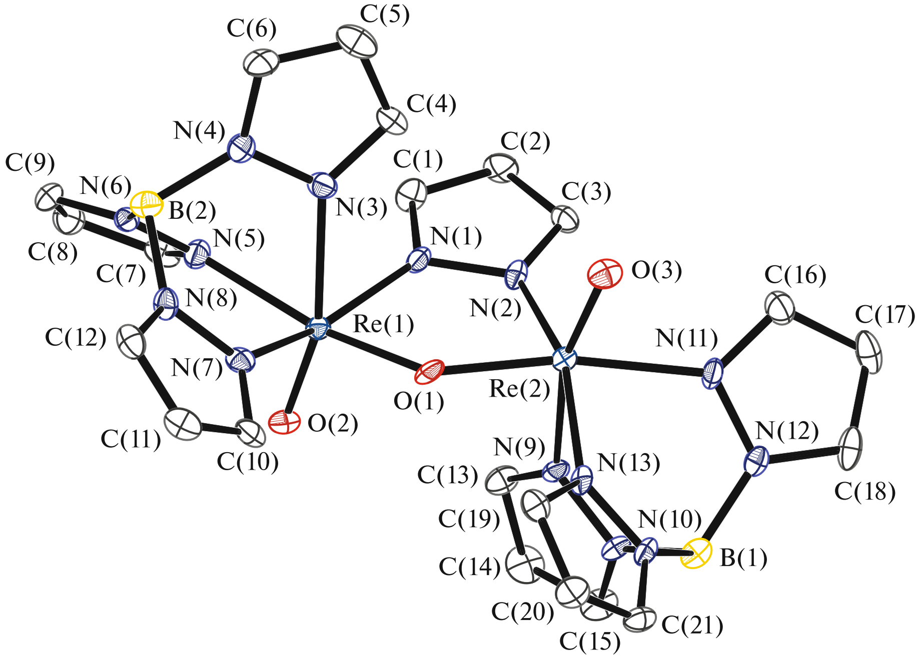

Fig. 3. Molecular structure of complex **III**. Selected bond lengths: Re(1)–O(1) 1.938(4), Re(1)–O(2) 1.676(4), Re(1)–N(1) 2.046(5), Re(1)–N(3) 2.248(5), Re(1)–N(5) 2.133(5), Re(1)–N(7) 2.071(5), Re(2)–O(1) 1.924(4), Re(2)–O(3) 1.688(4), Re(2)–N(2) 2.055(5), Re(2)–N(9) 2.237(5), Re(2)–N(11) 2.159(5), and Re(2)–N(13) 2.067(5) Å and bond angles: Re(2)O(1)Re(1) 130.5(2)°, O(2)Re(1)O(1) 105.3(2)°, O(2)Re(1)N(1) 103.8(2)°, O(3)Re(2)O(1) 105.7(2)°, and O(3)Re(2)N(2) 100.2(2)°.

The theoretical calculation of the rotation barrier in complex **I** by the density functional theory gives a lower value (8.2 kcal/mol) than those for the thiolate complexes (14.1 and 12.3 kcal/mol). Unlike the thiolate complexes, the Re–O bond with the rotating OMe group does not elongate in the transition state, but the $ReOC_{Me}$ angle increases to 140°. This fact assumes that a decrease in the rotation barrier on going from sulfur to oxygen is mainly related to a possibility of an additional donation of two lone pairs on the oxygen to the antibonding π orbitals of the multiple Re–O bond with terminal oxygen regardless of the dihedral $OReOC_{Me}$ angle. At the same time, an electron pair with the *s* character is not almost involved in the additional Re–S bonding in the case of sulfur.

No NMR spectra of complex **II** were detected because of the very low solubility in usual deuterated solvents. A colorless solution is formed on heating complex **II** to 80°C in DMSO-d_6. The NMR spectrum of this solution contains a broadened singlet of the BH fragment (3.37 ppm) and one set of signals from the pyrazolate ring (6.53, 8.18, and 8.37 ppm). It is most likely that the complex is oxidized with DMSO to $TpReO_3$ [24] similarly to the formation of $(Pz_4B)ReO_3$ in the reaction of $[(Pz_4B)ReO_2]_2$ with DMSO [4].

The reaction of complex **I** with carboxylic acids (AcOH, PhCOOH) results in the formation of complex **II** only in a low yield possibly due to the reaction with water traces. The reaction of complex **I** with an acetic anhydride excess results in the substitution of the methylate substituents by acetates to form complex **IV**.

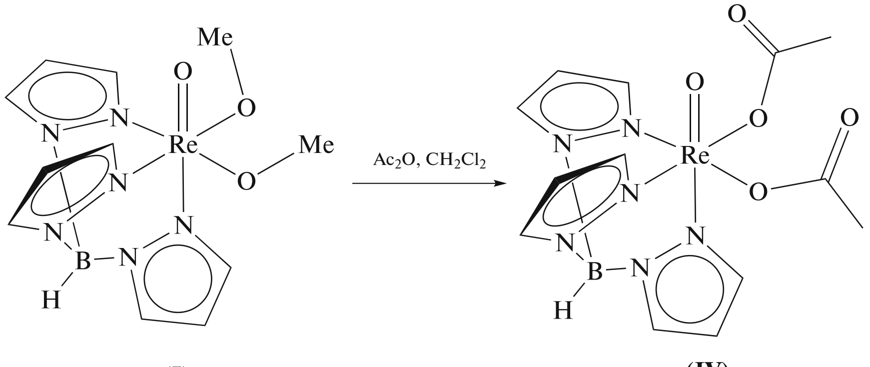

(I) **(IV)**

Scheme 3.

The IR spectrum of complex **IV** exhibits two bands of asymmetric vibrations of carboxylate groups at 1686 and 1661 cm^{-1}, which are absent from the spectrum of the starting complex. The bands of the OCO symmetric vibrations are observed, most likely, at 1284 and 1244 cm^{-1}, but their assignment is less evident, since the intense bands in this range are also observed in the spectrum of the starting complex. The band of B–H vibrations shifts from 2518 to 2539 cm^{-1} on going from complex **I** to **IV**, most likely, due to differences in the crystal packings: in the crystal of complex **I** the B–H bond is directed toward the π system of one of the pyrazolate rings of the adjacent molecule, whereas in complex **IV** the B–H bond is directed between the oxygen atoms of the acetate groups (HB...O 2.89, 3.12 Å). As for complex **I**, the ^{1}H and ^{13}C NMR spectra of complex **IV** exhibit one signal of the methyl groups and two sets of signals of pyrazolates in a ratio of 1 : 2 showing an equivalence of the acetate substituents in the solution.

According to the XRD data, in complex **IV** (Fig. 4) the acetate groups are coordinated by one oxygen atom only with a noticeable symmetry of the C–O distances for the oxygen atoms bound to rhenium (1.273(4), 1.331(4) Å) and not bound to it (1.236(5), 1.216(4) Å). The Re–O bonds with the acetate groups (2.005(2), 1.976(2) Å) are longer than the Re–O bonds with the methylate groups (1.969(5), 1.933(5) Å) in complexes **I**, and the Re–N distances for the nitrogen atoms in the *trans* position to the acetate groups (2.069(2), 2.098(2) Å) and the Re–O distance with the oxo ligand (1.669(2) Å) are somewhat shortened compared to similar distance in complex **I**. These specific features of the geometry indicate a weaker binding of rhenium with acetates compared to methylates in such complexes, which is consistent with a lower resistance of complex **IV** to hydrolysis and the fact that compound **IV** cannot be synthesized by the exchange reaction of complex **I** with acetic acid.

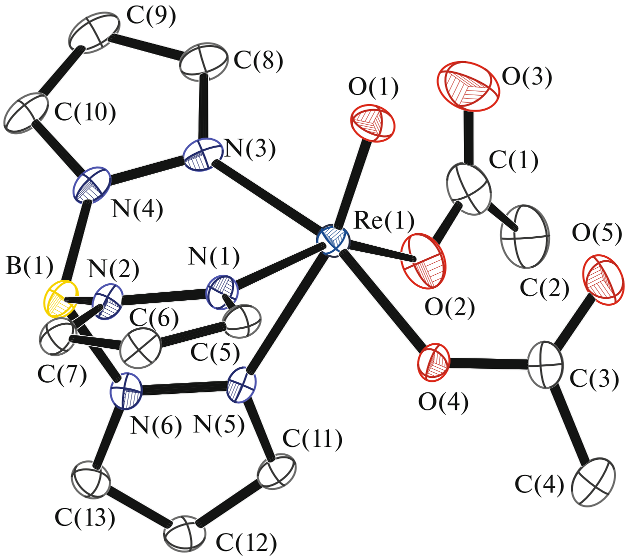

Fig. 4. Molecular structure of complex **IV**. Selected bond lengths: Re(1)–O(1) 1.669(2), Re(1)–O(2) 2.005(2), Re(1)–O(4) 1.976(2), Re(1)–N(1) 2.069(2), Re(1)–N(3) 2.098(2), Re(1)–N(5) 2.255(2), O(2)–C(1) 1.273(4), O(3)–C(1) 1.236(5), O(4)–C(3) 1.331(4), and O(5)–C(3) 1.216(4) Å and bond angles: O(1)Re(1)O(2) 111.0(1)°, O(1)Re(1)O(4) 105.9(1)°, O(4)Re(1)O(2) 82.9(1)°, C(1)O(2)Re(1) 130.8(3)°, and C(3)O(4)Re(1) 124.2(2)°.

ACKNOWLEDGMENTS

The studies were carried out using the equipment of the Center for Collective Use of Physical Methods of Investigation at the Kurnakov Institute of General and Inorganic Chemistry (Russian Academy of Sciences).

FUNDING

This work was supported by the Russian Science Foundation, project no. 18-73-10206.

CONFLICT OF INTEREST

The authors declare that they have no conflicts of interest.

REFERENCES

1. Trofimenko, S., *Chem. Rev.*, 1993, vol. 93, p. 943.
2. Calogero, S., Lobbia, G.G., Cecchi, P., et al., *Polyhedron*, 1994, vol. 13, p. 87.
3. Lail, M., Pittard, K.A., and Gunnoe, T.B., *Adv. Organomet. Chem.*, 2008, vol. 56, p. 95.
4. Paulo, A., Domingos, A., Marcalo, J., et al., *Inorg. Chem.*, 1995, vol. 34, p. 2113.
5. Nunes, D., Domingos, A., Paulo, A., et al., *Inorg. Chim. Acta*, 1998, vol. 271, p. 65.
6. Lassen, P.R., Guy, L., Karame, I., et al., *Inorg. Chem.*, 2006, vol. 45, p. 10230.
7. Klüfers, P., Krotz, O., and Oßberger, M., *Eur. J. Inorg. Chem.*, 2002, p. 1919.
8. Brown, S.N. and Mayer, J.M., *J. Am. Chem. Soc.*, 1996, vol. 118, p. 12119.
9. Brown, S.N. and Mayer, J.M., *Inorg. Chem.*, 1992, vol. 31, p. 4091.
10. Middleditch, M., Anderson, J.C., Blake, A.J., and Wilson, C., *Inorg. Chem.*, 2007, vol. 46, p. 2797.
11. Abrams, M.J., Davison, A., and Jones, A.G., *Inorg. Chim. Acta*, 1984, vol. 82, p. 125.
12. *SADABS. Version 2008/1*, Madison: Bruker AXS Inc., 2008.
13. Sheldrick, G.M., *Acta Crystallogr., Sect. A: Found. Crystallogr.*, 2008, vol. 64, p. 112.
14. Dolomanov, O.V., Bourhis, L.J., Gildea, R.J., et al., *J. Appl. Crystallogr.*, 2009, vol. 42, p. 339.
15. Neese, F., *WIREs Comput. Mol. Sci.*, 2012, vol. 2, p. 73.
16. Perdew, J.P., Burke, K., and Ernzerhof, M., *Phys. Rev. Lett.*, 1996, vol. 77, p. 3865.
17. Perdew, J.P., Burke, K., and Ernzerhof, M., *Phys. Rev. Lett.*, 1997, vol. 78, p. 1396.
18. Weigend, F. and Ahlrichs, R., *Phys. Chem. Chem. Phys.*, 2005, vol. 7, p. 3297.
19. Grimme, S., Ehrlich, S., and Goerigk, L., *J. Comput. Chem.*, 2011, vol. 32, p. 1456.
20. Grimme, S., Antony, J., Ehrlich, S., and Krieg, H., *J. Chem. Phys.*, 2010, vol. 132, p. 154104.
21. Adamo, C. and Barone, V., *J. Chem. Phys.*, 1999, vol. 110, p. 6158.
22. Cordero, B., Gómez, V., Platero-Prats, A.E., et al., *Dalton Trans.*, 2008, vol. 21, p. 2832.
23. Skabitskii, I.V., Sakharov, S.G., Pasynskii, A.A., and Eshmakov, R.S., *Russ. J. Coord. Chem.*, 2019, vol. 45, no. 8, p. 539.
24. Degnan, I.A., Herrmann, W.A., and Herdtweck, E., *Chem. Ber.*, 1990, vol. 123, p. 1347.

Translated by E. Yablonskaya